

Resolution of Tissue Microstructure via Diffusion MR: Beyond Mapping Orientations

Evren Özarslan

Section on Tissue Biophysics and Biomimetics
NICHD, National Institutes of Health



- **Single-PFG**

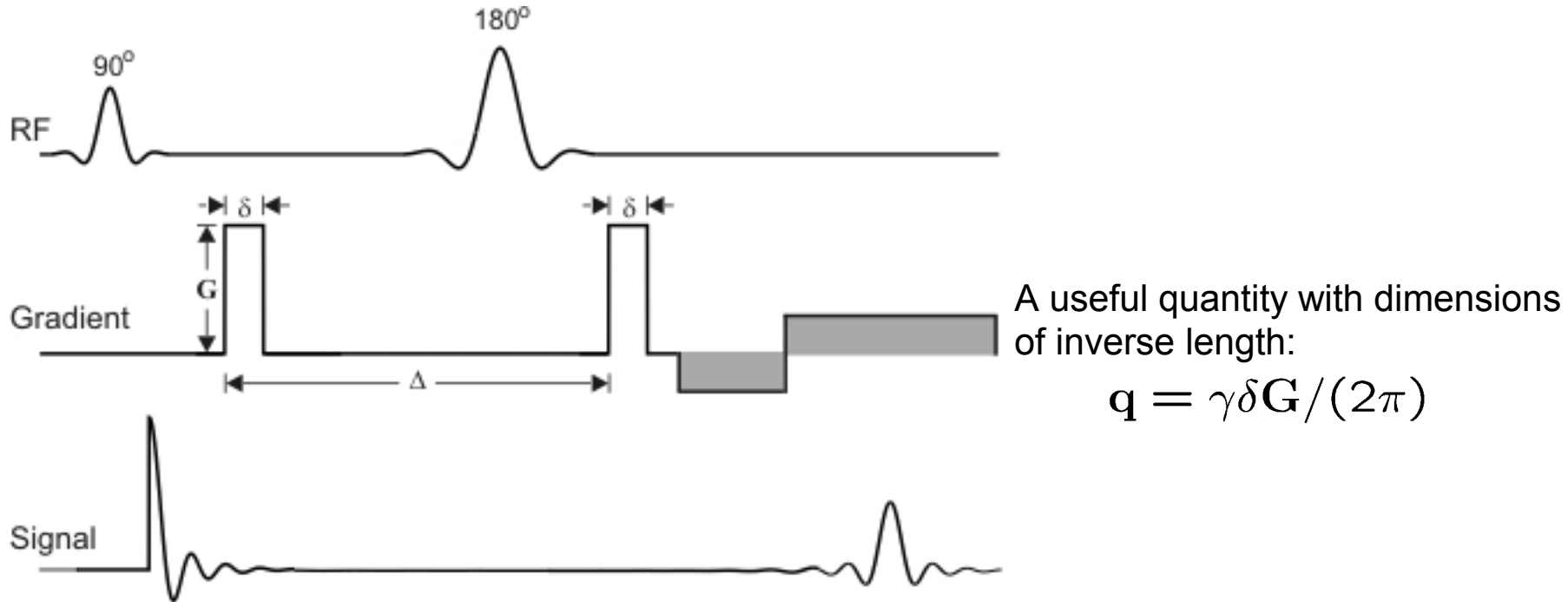
- **From geometry to MR signal**
- **Restricted diffusion**
- **Signal to Geometry**
- **Tissue as disordered medium**

- **Double-PFG**

- **Diffraction measurements**
- **Anisotropy at different length scales**
- **General theory of diffusion attenuation**

- **Conclusion**

Diffusion-Weighted MR Imaging (DWI)



When δ is small, MR signal attenuation (S/S_0) is given by

$$E_{\Delta}(\mathbf{q}) = \int d\mathbf{r} \rho(\mathbf{r}) \int d\mathbf{r}' P_{\Delta}(\mathbf{r}, \mathbf{r}') \exp(i2\pi \mathbf{q} \cdot (\mathbf{r} - \mathbf{r}'))$$

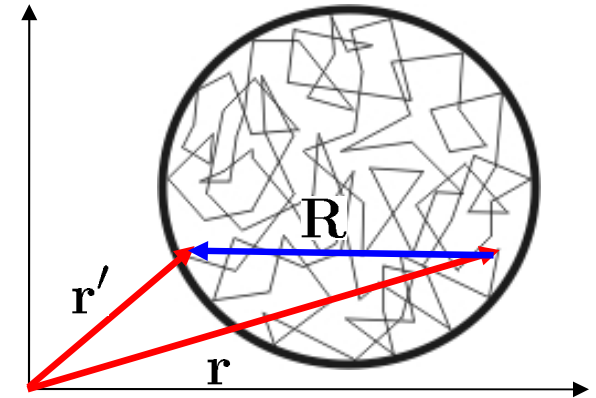
Initial spin density

Propagator (Gaussian for free diffusion; depends on the pore shape and size for restricted diffusion)

The Ensemble Average Propagator

$$E_{\Delta}(\mathbf{q}) = \int d\mathbf{r} \rho(\mathbf{r}) \int d\mathbf{r}' P_{\Delta}(\mathbf{r}, \mathbf{r}') \exp(i2\pi\mathbf{q} \cdot (\mathbf{r} - \mathbf{r}'))$$

Probability that a molecule at \mathbf{r} during the application of the first pulse will end up at \mathbf{r}' during the application of the second pulse.



Let's introduce a new variable: $\mathbf{R} = \mathbf{r}' - \mathbf{r}$

$$E_{\Delta}(\mathbf{q}) = \int d\mathbf{r} \rho(\mathbf{r}) \int d\mathbf{R} P_{\Delta}(\mathbf{r}, \mathbf{R}) \exp(-i2\pi\mathbf{q} \cdot \mathbf{R})$$

$$E_{\Delta}(\mathbf{q}) = \int d\mathbf{R} \exp(-i2\pi\mathbf{q} \cdot \mathbf{R}) \underbrace{\int d\mathbf{r} \rho(\mathbf{r}) P_{\Delta}(\mathbf{r}, \mathbf{R})}_{\overline{P}_{\Delta}(\mathbf{R})} \quad \leftarrow \text{EAP}$$

$$P_{\Delta}(\mathbf{R}) = \int d\mathbf{q} \exp(i2\pi\mathbf{q} \cdot \mathbf{R}) E_{\Delta}(\mathbf{q})$$

- Find the propagator, then integrate:

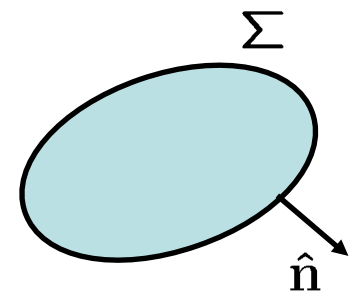
$$E_{\Delta}(\mathbf{q}) = \int d\mathbf{r} \rho(\mathbf{r}) \int d\mathbf{r}' P_{\Delta}(\mathbf{r}, \mathbf{r}') \exp(i2\pi \mathbf{q} \cdot (\mathbf{r} - \mathbf{r}'))$$

- The propagator satisfies

- the diffusion equation $D_0 \nabla'^2 P_t(\mathbf{r}, \mathbf{r}') = \frac{\partial P}{\partial t}$

- the initial condition $P_0(\mathbf{r}, \mathbf{r}') = \delta(\mathbf{r} - \mathbf{r}')$

- the boundary condition $\hat{\mathbf{n}} \cdot \nabla P_t(\mathbf{r}, \mathbf{r}')|_{\mathbf{r} \in \Sigma} = 0$

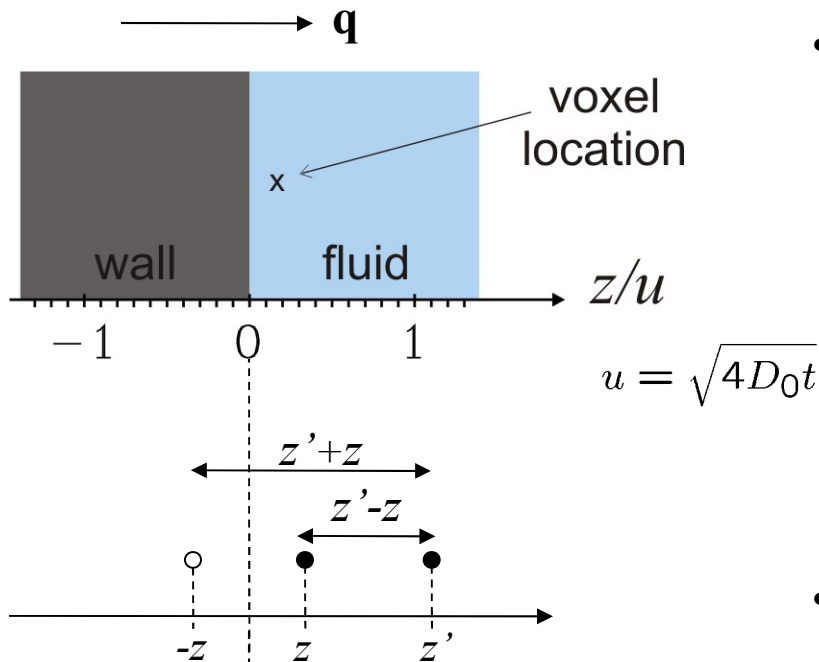


No Boundaries? (Free diffusion)

- Propagator is a Gaussian $P_t(\mathbf{r}, \mathbf{r}') = \frac{1}{(4\pi D_0 t)^{3/2}} \exp\left(-\frac{|\mathbf{r} - \mathbf{r}'|^2}{4D_0 t}\right)$

- Signal is another Gaussian $E_t(\mathbf{q}) = \exp(-4\pi^2 |\mathbf{q}|^2 D_0 t)$

Method of Images



- This is a one-dimensional problem:

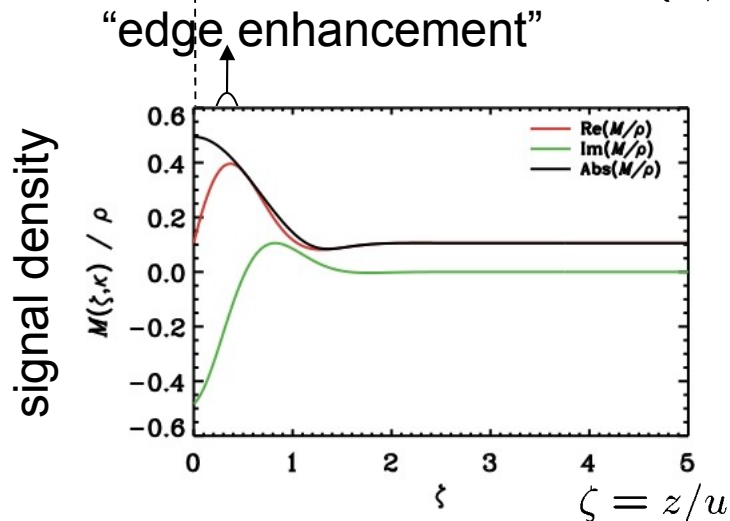
$$D_0 \frac{\partial^2 P_t(z, z')}{\partial z'^2} = \frac{\partial P}{\partial t}$$

$$P_0(z, z') = \delta(z - z')$$

$$\left. \frac{\partial P_t(z, z')}{\partial z} \right|_{z=0} = 0$$

- The propagator can be written as:

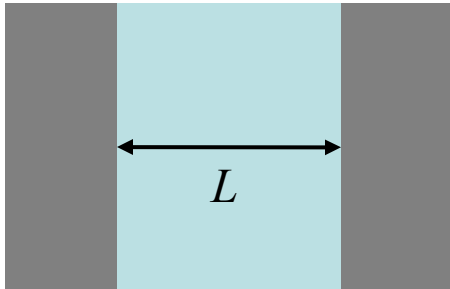
$$P_t(z, z') = \frac{1}{\sqrt{\pi}u} \left(e^{-(z'-z)^2/u^2} + e^{-(z'+z)^2/u^2} \right) \times \Theta(z) \Theta(z')$$



A truly bi-Gaussian function !

→ Diffusion signal is complex valued !

Two parallel plates



- **Method of images** can still be applied:

$$P_t(z, z') = \frac{1}{\sqrt{4\pi D_0 t}} \sum_{n=-\infty}^{\infty} \left[e^{-(2nL+z-z')^2/(4D_0 t)} + e^{-(2nL+z'+z)^2/(4D_0 t)} \right]$$

Infinitely many images

- An alternative: **Eigenfunction expansion**

$$P_t(\mathbf{r}, \mathbf{r}') = \sum_{n=0}^{\infty} e^{-\lambda_n t} u_n(\mathbf{r}) u_n^*(\mathbf{r}')$$

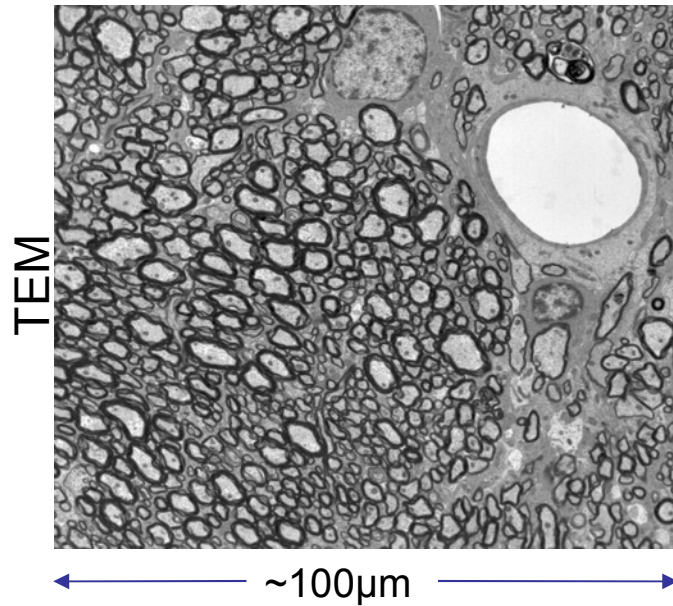
where $-D_0 \nabla^2 u_n(\mathbf{r}) = \lambda_n u_n(\mathbf{r})$

- The eigenfunctions have to satisfy the boundary conditions as well.

$$u_n(z) \propto \cos \frac{n\pi z}{L} \qquad \frac{\lambda_n}{D_0} = \frac{n^2 \pi^2}{L^2}$$

- Comparing the two forms of the (same) propagator, it is clear that the first form of the propagator is more efficient at short diffusion times, whereas the second is more appropriate at long diffusion times.

From Signal to Geometry



- Cohesion is important.

Experimental Design

Analytical Methods

Examined Tissue

- The kind of information that can be obtained:
 - Cell size
 - Cell shape
 - Intracellular and extracellular volume fractions
 - Tortuosity
 - Membrane permeability
 - ...
 - Distributions of the above

- E.g., if one is interested in measuring a cell size of 3 μm, a pulse duration of 1 ms is too long.

- What matters is the ratio $\frac{6D_0\delta}{a^2}$
(=0.67 for $D_0=1\times10^{-3}$ mm²/s)

- Solution:

- Use significantly shorter gradient pulses
- Incorporate the pulse width into theory

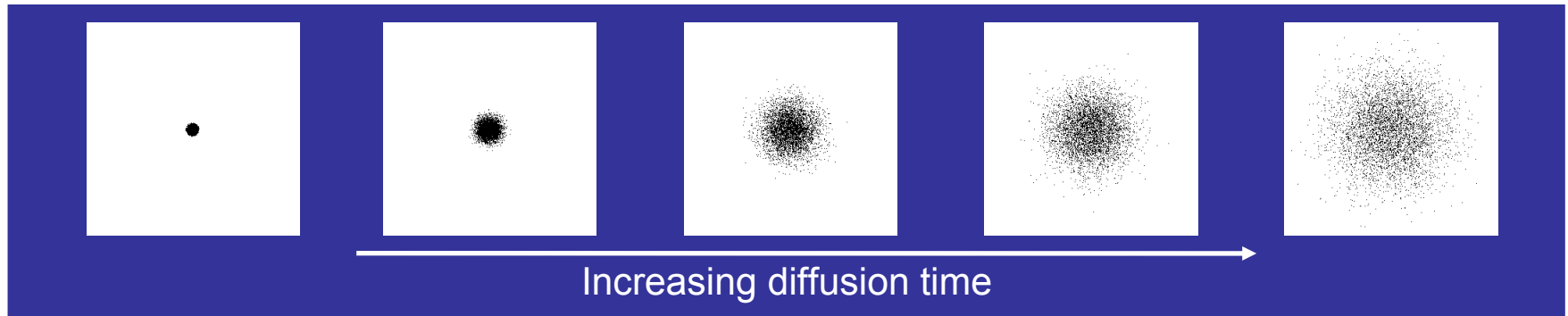


*“Clouds are not spheres, mountains are not cones,
coastlines are not circles, bark is not smooth, nor does
lightning travel in a straight line.”*

Mandelbrot B. *Fractal Geometry of Nature*, Freeman, 1982.

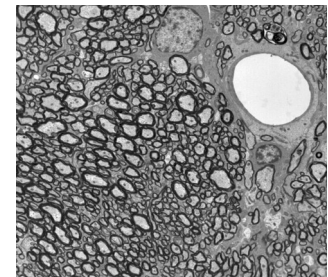
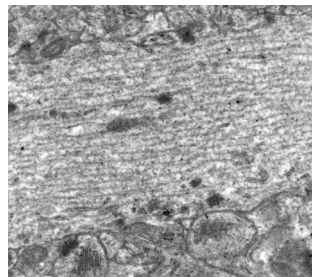
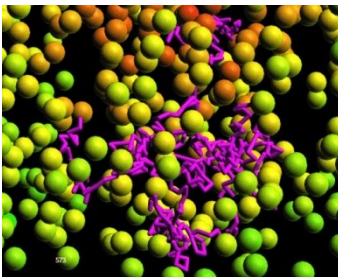
Probing Different Length Scales via MR

- It is possible to probe different length scales using diffusion-weighted MR by adjusting the diffusion time (Δ).



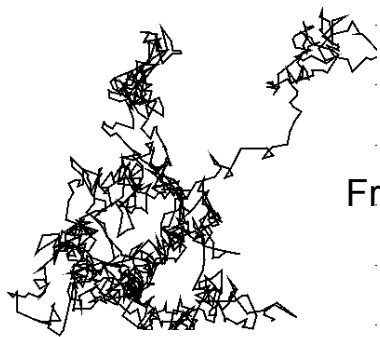
- Typical range of distances that can be probed is: 0.25-7 μm .

Lipman et al.
Cover of
Computational
Materials
Science, 1995.



- Water molecules in neural tissue is restricted by macromolecules, cellular organelles, and cytoskeletal proteins, by the complex shapes of nervous tissue cells, and by the complex spatial arrangements of neurons and glia in tissue.

Diffusion Time Dependence



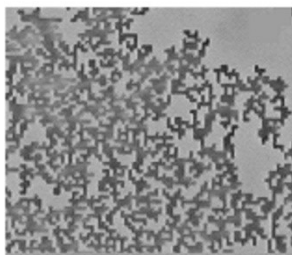
Free diffusion



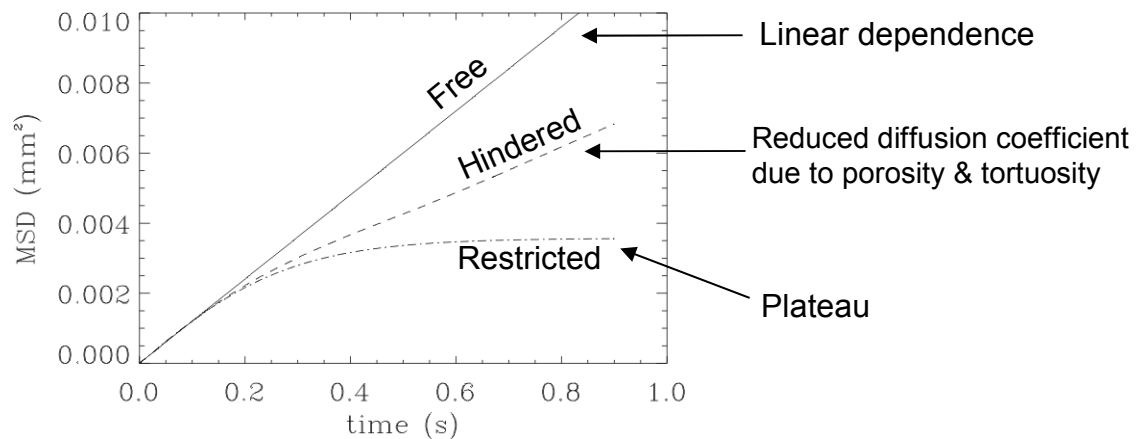
Hindered diffusion



Restricted diffusion

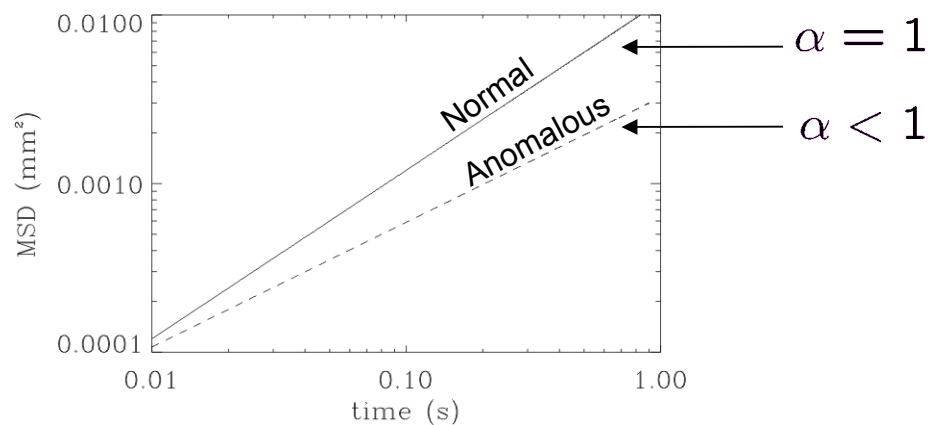


Anomalous diffusion

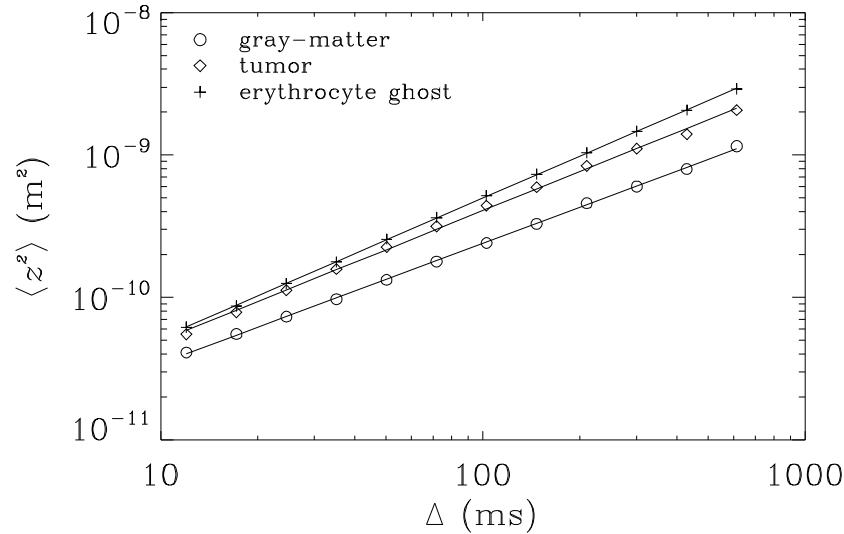
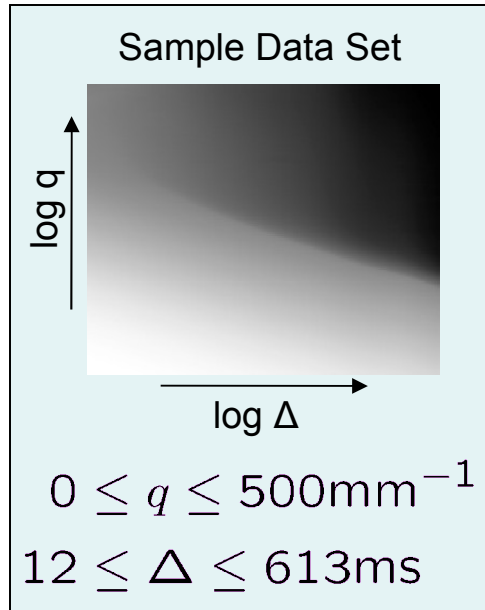


- Let's look at the double logarithmic plots.
- Power-laws yield straight lines in log-log plots.

$$\text{MSD} \propto t^\alpha \longrightarrow \text{slope} = \alpha$$



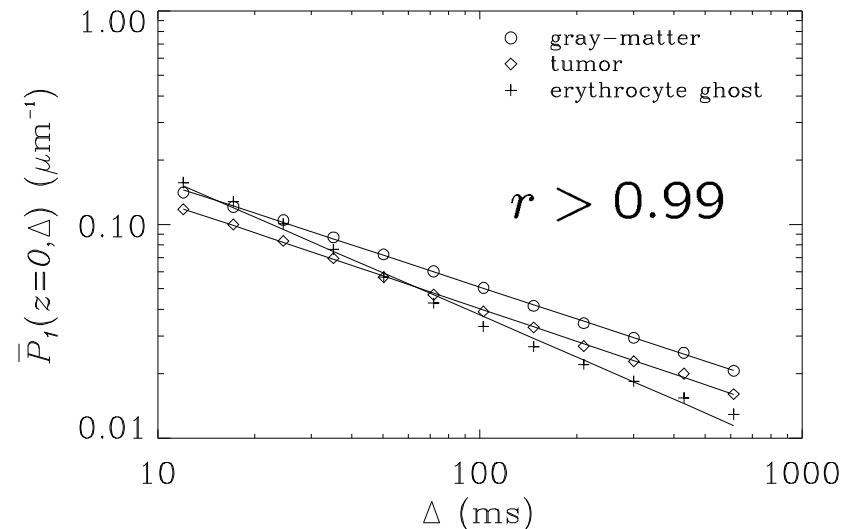
Observation of Anomalous Diffusion*



$$\text{MSD} = \langle z^2 \rangle \propto \Delta^{2/d_w}$$

$$r > 0.999$$

$$P_1(z=0, \Delta) \propto \Delta^{-d'_s/2}$$

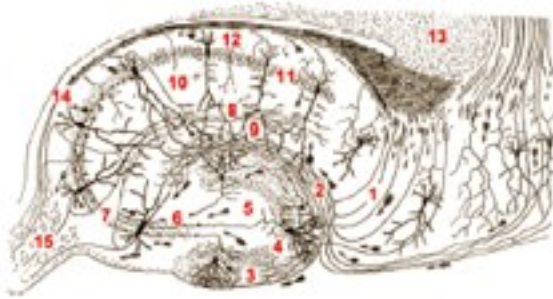


- These scaling laws were tested on different data sets.
- Diffusion in neural tissue appears to be anomalous and in the subdiffusive regime.

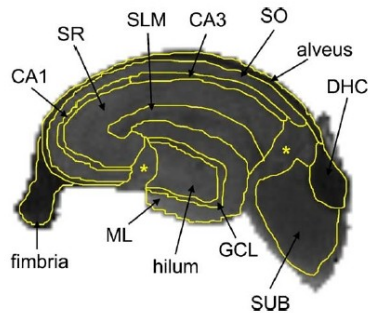
	d_w	d_s
Gray-matter	2.371	3.166
Tumor	2.189	1.909
Erythrocyte ghosts	2.036	4.852

* Özarslan et al., J Magn Reson, 183, p. 315, 2006.

Novel Image Contrast ?



Cajal, 1911. Histologie Du Systeme Nerveux De L'Homme Et Des Vertebres. A. Maloine, Paris.

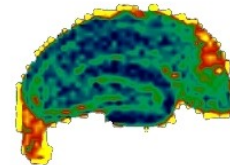


Shepherd et al., Neurolmage, 32, p.1499, 2006.

Anomalous

Traditional

d_w



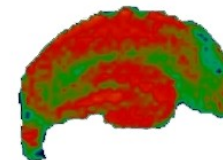
DWI

d'_s



MD

d'_f



FA

Özarslan et al., In Proc. Intl. Soc. Mag. Reson. Med. 15. p. 819, 2007.

Outline

- **Single-PFG**

- From geometry to MR signal
- Restricted diffusion
- Signal to Geometry
- Tissue as disordered medium

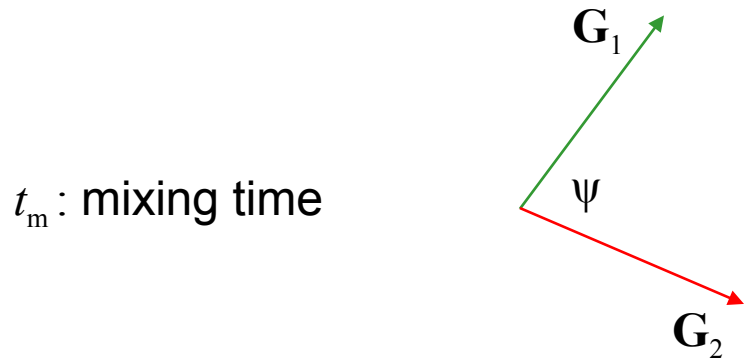
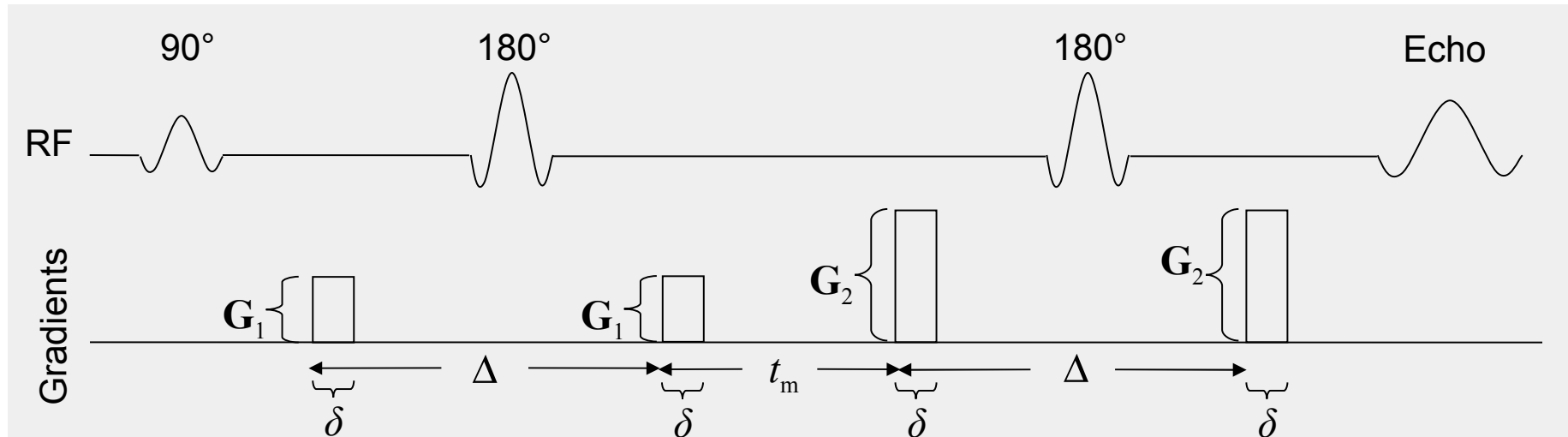
- **Double-PFG**

- Diffraction measurements
- Anisotropy at different length scales
- General theory of diffusion attenuation

- **Conclusion**

Double Pulsed Field Gradient (PFG) MR

- The problem with single-PFG: The data are featureless.
 - One can fit many different models to essentially the same data



For simplicity, all δ 's and Δ 's are taken to be the same.

Related Work

➤ Some of the works related to restricted diffusion:

➤ Mitra, Phys Rev B 51 (1995) p. 15074.

➤ Mitra's treatment considered only special limiting cases of the double-PFG experiment:

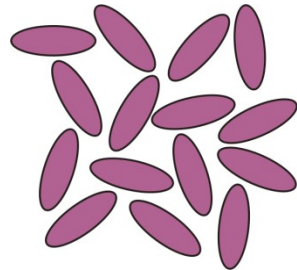
$$|G_1| = |G_2|$$

$$\Delta \rightarrow \infty$$

$$\delta = 0$$

$$t_m = 0 \quad \text{or} \quad t_m \rightarrow \infty$$

$$\gamma \delta G a \ll 1$$



isotropically
distributed pores

❖ Mitra's results were employed in:

- ❖ Cheng & Cory, JACS, 121 (1999) p. 7935.
- ❖ Komlosh et al., JMR, 189 (2007) p. 38.
- ❖ Komlosh et al., MRM, 59 (2008) p.803.
- ❖ Koch & Finsterbusch, MRM, 60 (2008) p. 90.
- ❖ Finsterbusch & Koch, JMR, 195 (2008) p. 23.
- ❖ Weber et al., Magn Reson Med, 61 (2009) p. 1001.

❖ Problems:

- ❖ Unavailability of a priori information
- ❖ More than one length scale within the pore
- ❖ Intravoxel heterogeneity
- ❖ Regional variations
- ❖ Effects of experimental parameters (pulse duration, imaging gradients, etc.) are not accounted for.

❖ General experimental parameters for accurate estimations

- ❖ Özarslan & Basser, J Chem Phys, 126 (2007) 154511.
- ❖ Shemesh et al., J Magn Reson, 198 (2009) p. 15.
- ❖ Özarslan et al., J Chem Phys, 130 (2009) 104702.
- ❖ Özarslan, J Magn Reson, 199 (2009) p. 56.
- ❖ Shemesh et al., J Magn Reson, 200 (2009) p. 214.

❖ Another signature of restricted diffusion via the diffusion-diffraction phenomenon

- ❖ Özarslan & Basser, J Magn Reson, 188 (2007) p. 285.

□ The predictions were verified by: Shemesh and Cohen, J Magn Reson, 195 (2008) p.153.

Signal in Diffraction Measurements

- Consider isolated pores and limiting cases of the experimental parameters

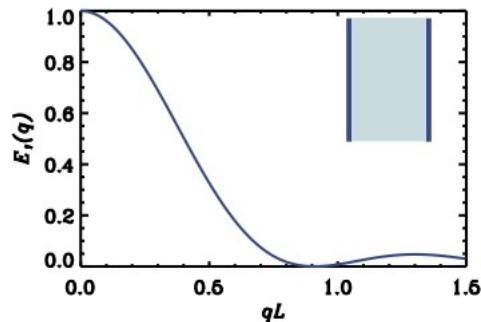
$$G_1 = G_2 = G, \quad \Delta \rightarrow \infty, \quad \delta = 0, \quad t_m = 0$$

- $\rho(\mathbf{r})$ is the pore indicator function, equal to a constant within the pore and vanishes elsewhere.

$$\tilde{\rho}(\mathbf{q}) = \int d\mathbf{r} \rho(\mathbf{r}) e^{-i2\pi\mathbf{q}\cdot\mathbf{r}}, \text{ where } \mathbf{q} = (2\pi)^{-1}\gamma\delta\mathbf{G}$$

Single-PFG

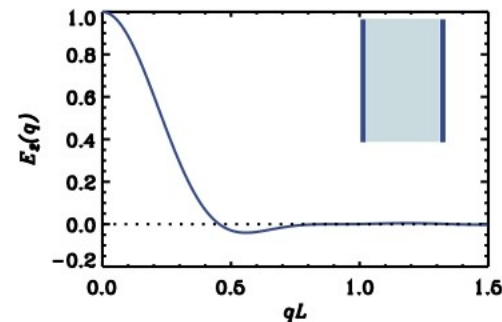
$$E(\mathbf{q}) = |\tilde{\rho}(\mathbf{q})|^2$$



- Non-monotonicity is a signature of restriction.

Double-PFG

$$E(\mathbf{q}) = \tilde{\rho}(\mathbf{q})^2 \tilde{\rho}(2\mathbf{q})^*$$

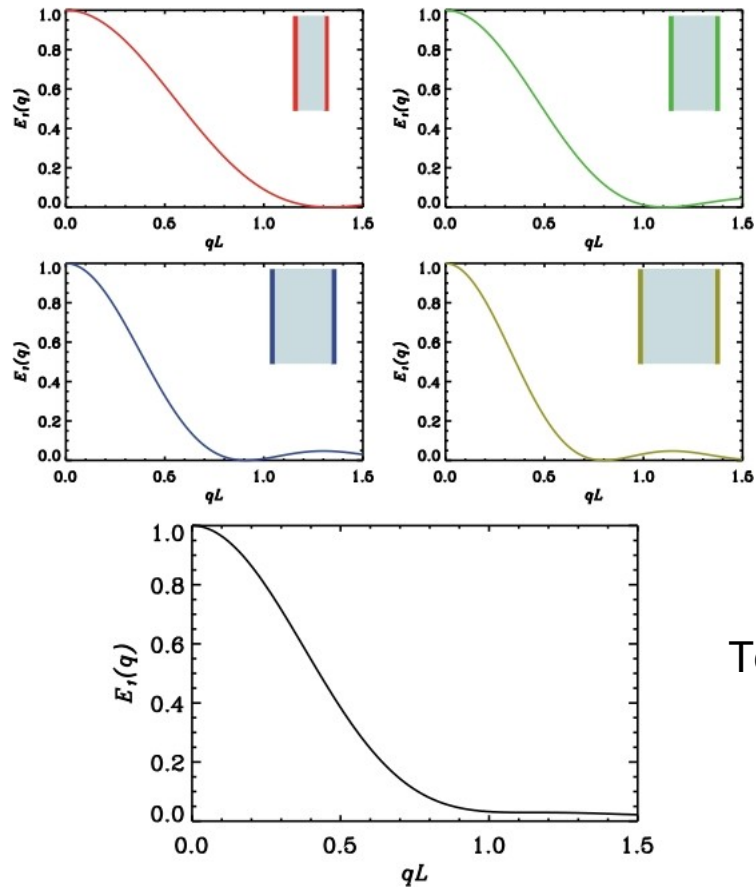


- Zero-crossing is a signature of restriction.

* Özarslan & Bassler, J Magn Reson, 188, p. 285, 2007.

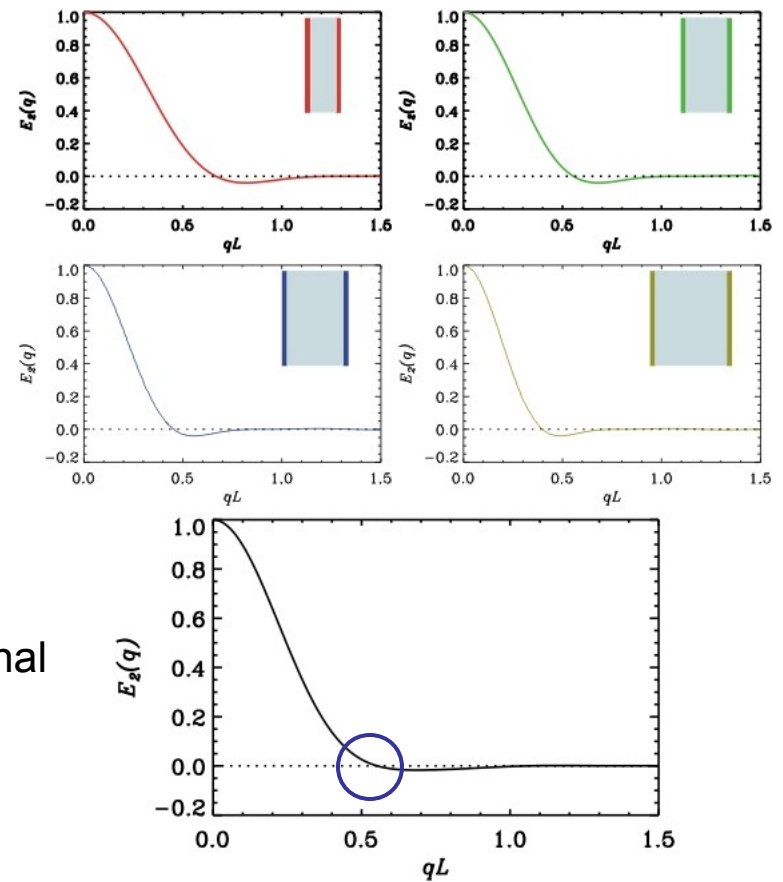
Heterogeneity and Diffraction Measurements

Single-PFG



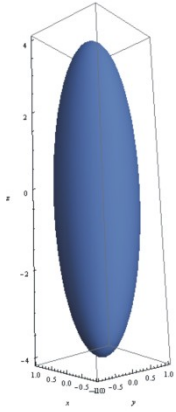
Nonmonotonicity is lost !

Double-PFG

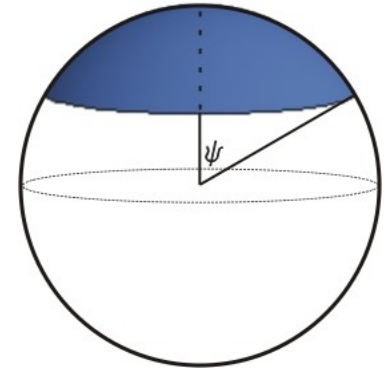


Zero-crossing is preserved !

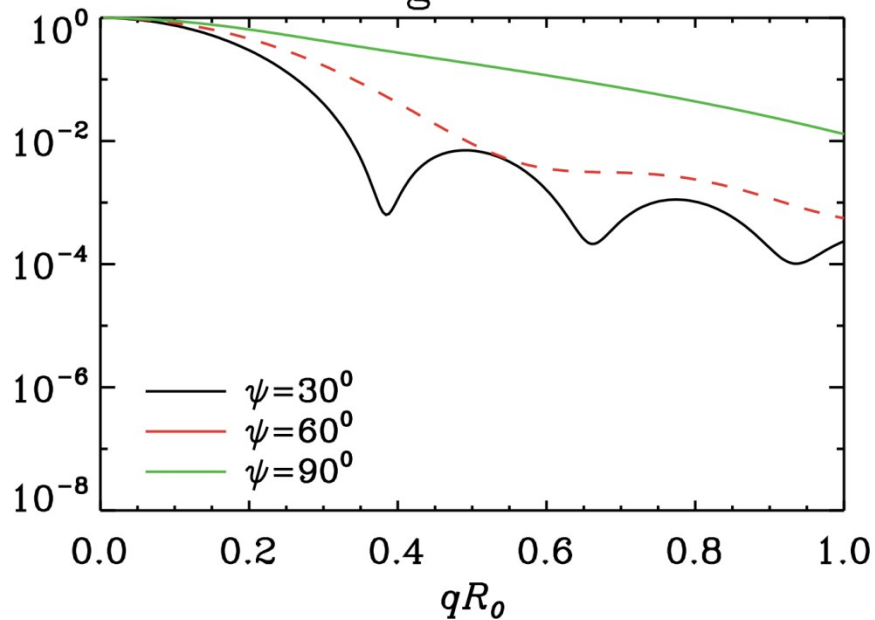
Orientational Heterogeneity and Diffraction Measurements



- Ellipsoids of semi-axes $a:b:c=1:1:4$ whose orientation vectors are uniformly distributed over a spherical cap.

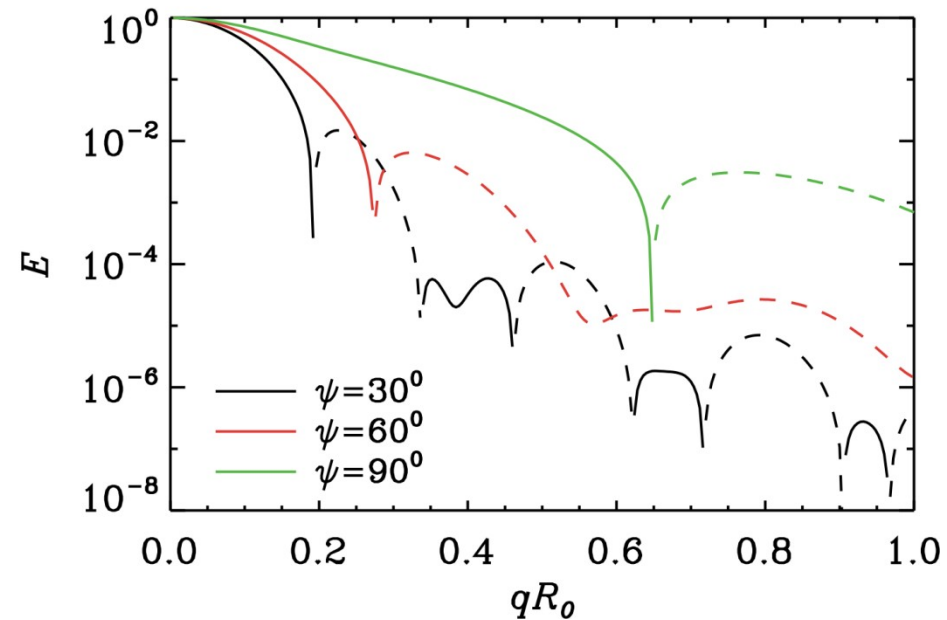


single-PFG



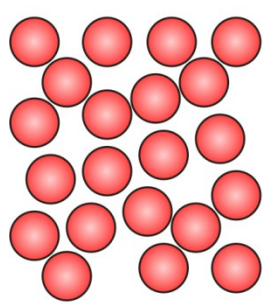
Nonmonotonicity is lost !

double-PFG

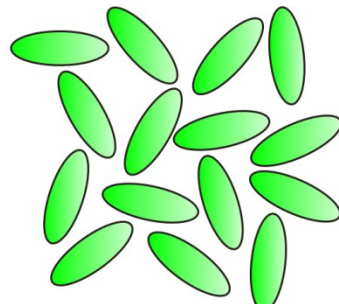


Zero-crossing is preserved !

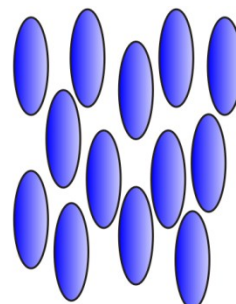
Anisotropy at Different Length Scales*



μA



$\mu A + CSA$



$\mu A + CSA + EA$

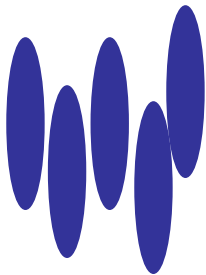
μA : microscopic anisotropy

CSA: compartment shape anisotropy

EA: ensemble anisotropy

Anisotropy in single-PFG acquisitions is compromised.

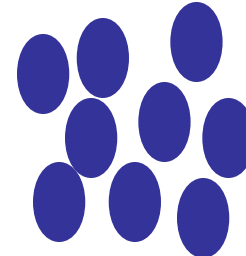
- Anisotropy is influenced by the coherence of the compartments.



High Anisotropy



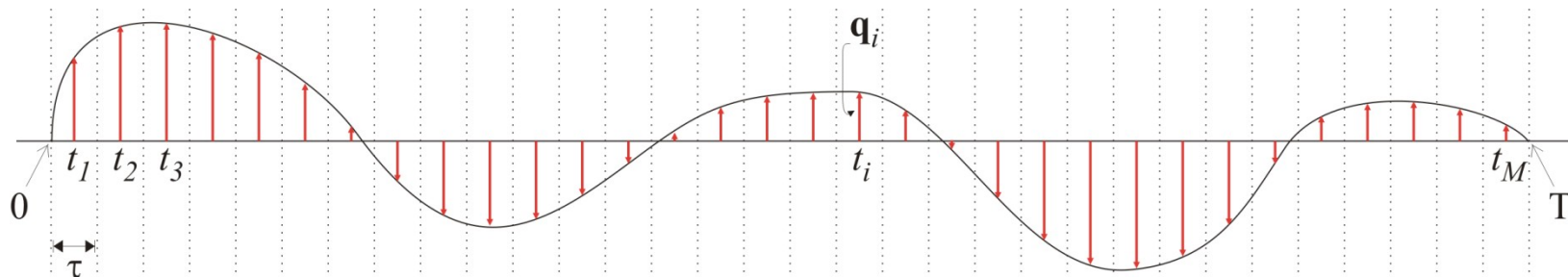
Low Anisotropy



Low Anisotropy

* Mitra, Phys Rev B, 51, 15074, 1995.

Signal as a Path Integral*



- ❖ Consider an **arbitrary pulse sequence**.
- ❖ Approximate it as a series of impulses.
 - Caprihan, Wang and Fukushima, J. Magn. Reson. A 118 (1996) p. 94.
- ❖ Write an approximation to the NMR signal intensity as a matrix product.
 - Callaghan, J. Magn. Reson. 129 (1997) p. 74.
- ❖ Collect the terms up to **quadratic** order.
- ❖ Take the limit of the resulting expression as $\tau \longrightarrow 0$, $M \longrightarrow \infty$ while $M\tau = T$.
- ❖ For D-dimensional isotropic pores:

$$E^{\text{rest}} \simeq 1 - 2\gamma^2 a^2 \sum_{n=1}^{\infty} s_{Dn} \int_0^T dt e^{\omega_{Dn} t} \mathbf{G}(t) \cdot \left(\int_t^T \mathbf{G}(t') e^{-\omega_{Dn} t'} dt' \right)$$

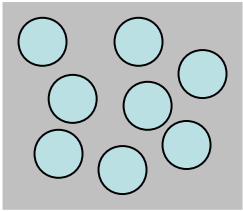
which is analogous to the free diffusion expression (Callaghan, Clarendon Press, Oxford, 1991).

$$E^{\text{free}} = \exp \left(-\gamma^2 D_0 \int_0^T dt \left| \int_0^t \mathbf{G}(t') dt' \right|^2 \right)$$

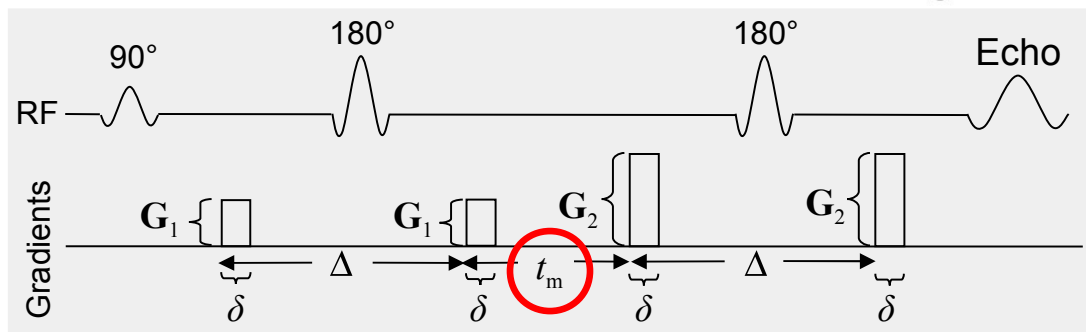
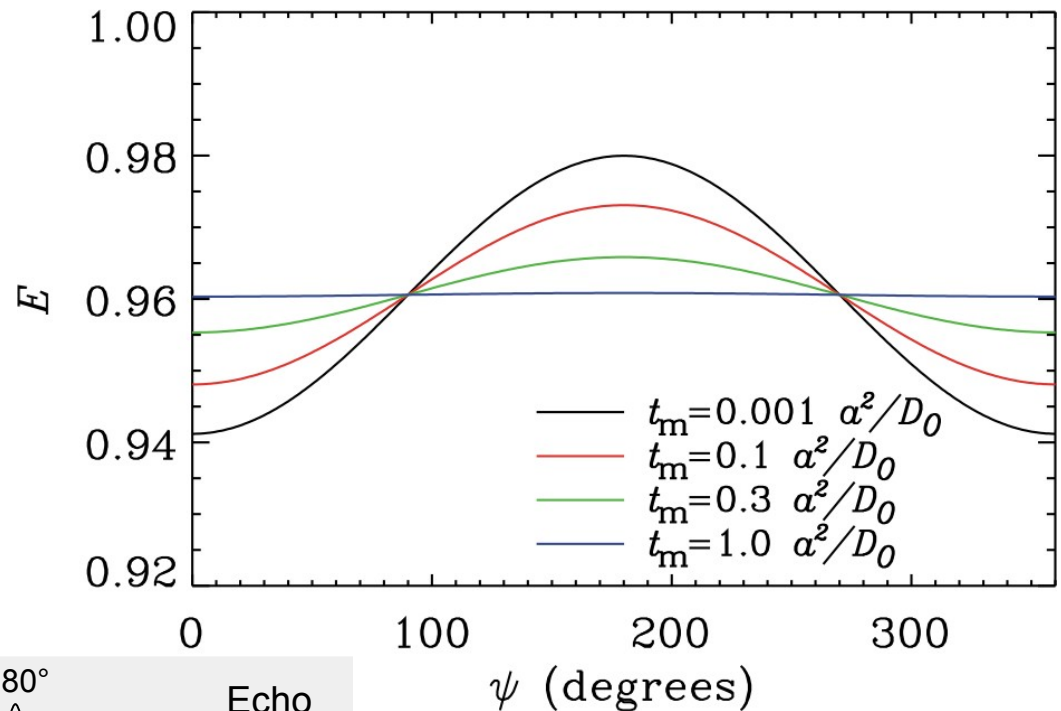
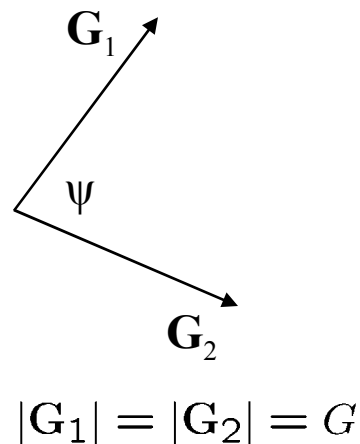
- ❖ Integrate for the double-PFG pulse sequence.

* Özarslan & Bassar, J Chem Phys, 128, 154511, 2008.

Predictions for double-PFG MR



- Microscopic anisotropy (a signature of restriction) influences the **low-q regime** for small mixing times !
- Simultaneous fiber direction and radius estimation may be possible using **clinical scanners**.



A General Solution

- MR signal for arbitrary pulse sequences can be obtained by tackling the Bloch-Torrey equation:

$$\frac{\partial M(\mathbf{r}, t)}{\partial t} = D_0 \nabla^2 M(\mathbf{r}, t) - i\gamma \mathbf{G}(t) \cdot \mathbf{r} M(\mathbf{r}, t)$$

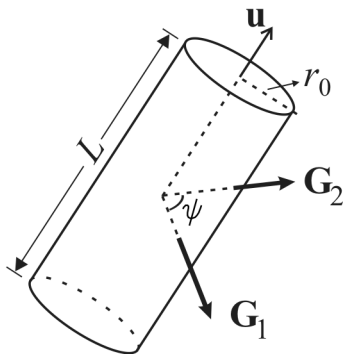
- A pseudo quantum mechanical approach:

- Robertson, Phys Rev 151 (1966) p. 273.
- Barzykin, Phys Rev B 58 (1998) p. 14171.
- Axelrod & Sen, J Chem Phys 114 (2001) p. 6878.
- Grebenkov, Rev Mod Phys 79 (2007) p. 1077.
- Grebenkov, J Chem Phys 128 (2008) p. 134702.
- Özarslan et al., J Chem Phys 130 (2009) p. 104702.

} MCF

→ MCF generalized to account for the variations in the direction of the gradient waveform

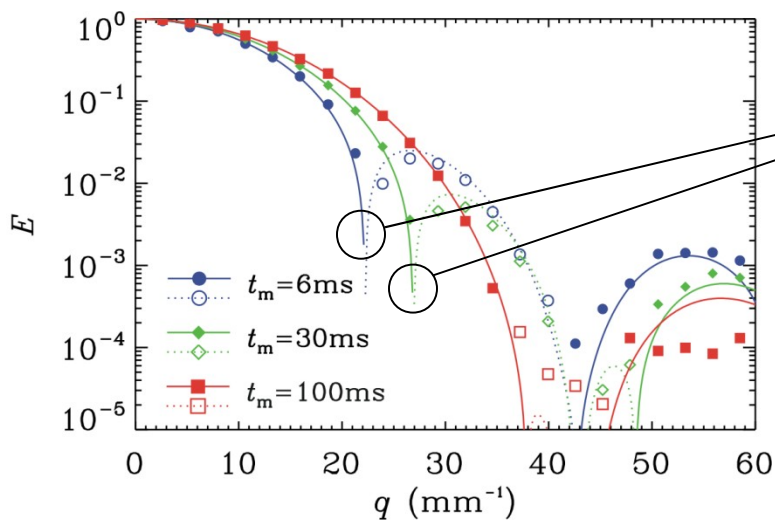
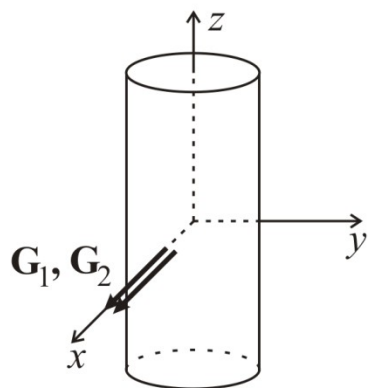
- The exact solution for the cylindrical geometry can be written as $E = E_{\parallel} E_{\perp}$



$$E_{\parallel} = \langle 0 | e^{-\Lambda_{\parallel} \delta + i 2 \pi q_{1\parallel} P} e^{-\Lambda_{\parallel} (\Delta - \delta)} e^{-\Lambda_{\parallel} \delta - i 2 \pi q_{1\parallel} P} e^{-\Lambda_{\parallel} (t_m - \delta)} e^{-\Lambda_{\parallel} \delta - i 2 \pi q_{2\parallel} P} e^{-\Lambda_{\parallel} (\Delta - \delta)} e^{-\Lambda_{\parallel} \delta + i 2 \pi q_{2\parallel} P} | 0 \rangle^*$$

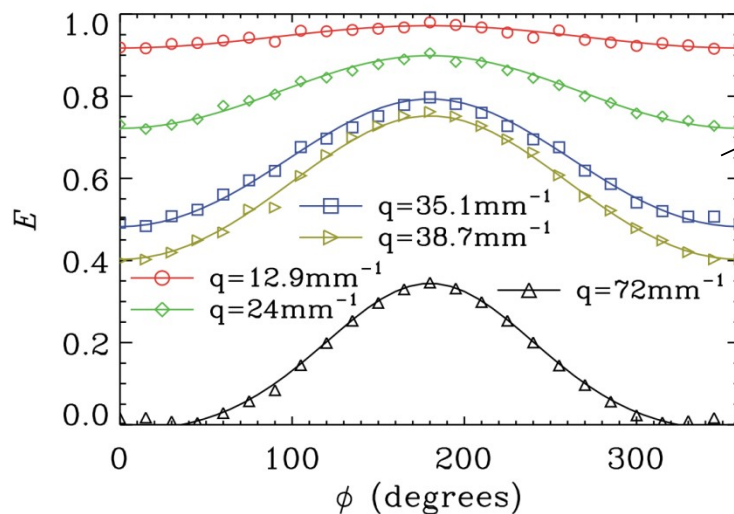
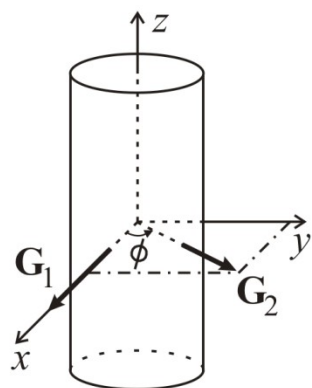
$$E_{\perp} = \langle 00 | e^{-\Lambda_{\perp} \delta + i 2 \pi q_{1a} T_a + i 2 \pi q_{1b} T_b} e^{-\Lambda_{\perp} (\Delta - \delta)} e^{-\Lambda_{\perp} \delta - i 2 \pi q_{1a} T_a - i 2 \pi q_{1b} T_b} e^{-\Lambda_{\perp} (t_m - \delta)} e^{-\Lambda_{\perp} \delta - i 2 \pi q_{2a} T_a - i 2 \pi q_{2b} T_b} e^{-\Lambda_{\perp} (\Delta - \delta)} e^{-\Lambda_{\perp} \delta + i 2 \pi q_{2a} T_a + i 2 \pi q_{2b} T_b} | 00 \rangle^*$$

Generalized MCF and Experimental Validation*



Zero-crossings*:

Robust to heterogeneity !



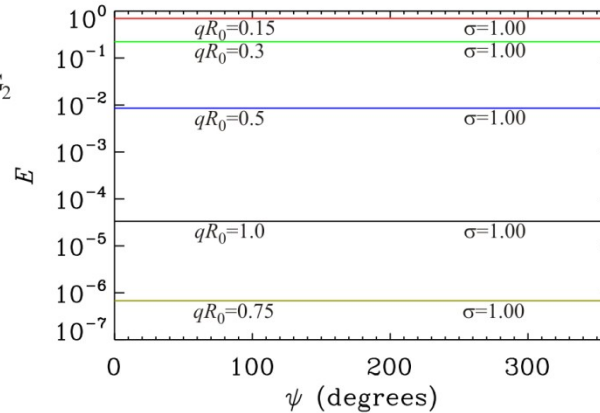
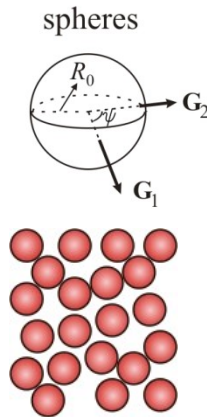
Microscopic anisotropy▪:

Probing restrictions at low gradient strengths !

* Unified framework: Özarslan et al., J Chem Phys 130 (2009) p. 104702.

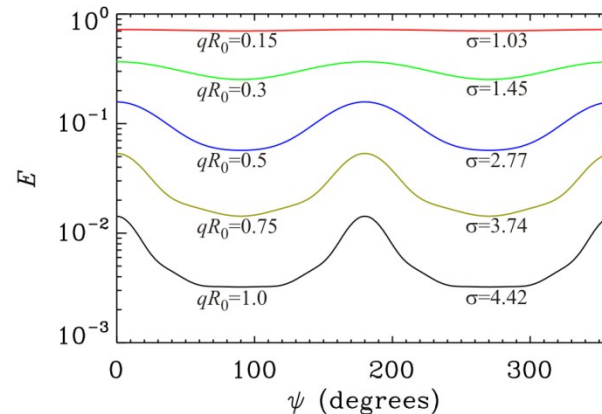
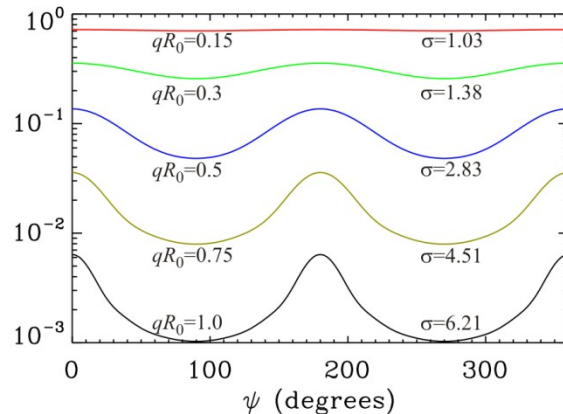
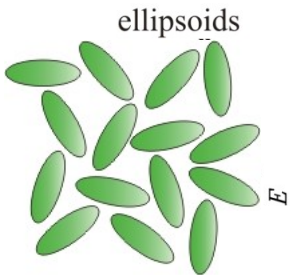
Resolution of Compartment Shape Anisotropy (CSA)*

$$t_m \rightarrow \infty$$



$$\mu = \frac{E(\psi = 180^\circ)}{E(\psi = 0^\circ)}$$

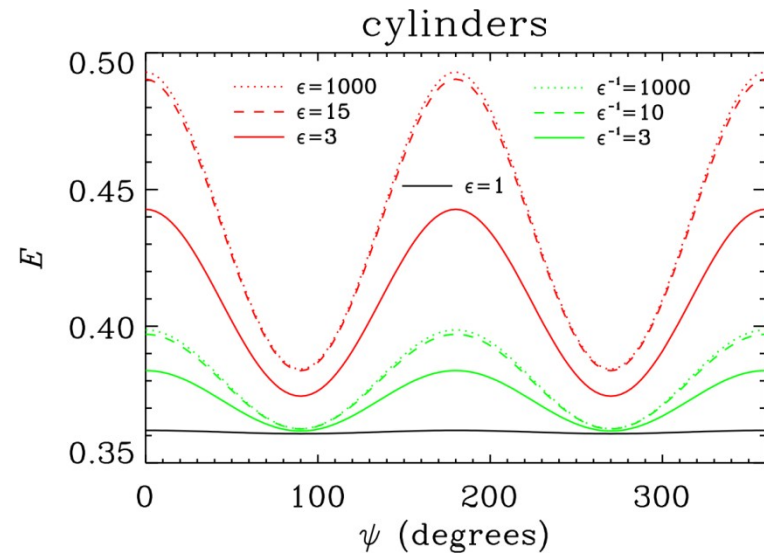
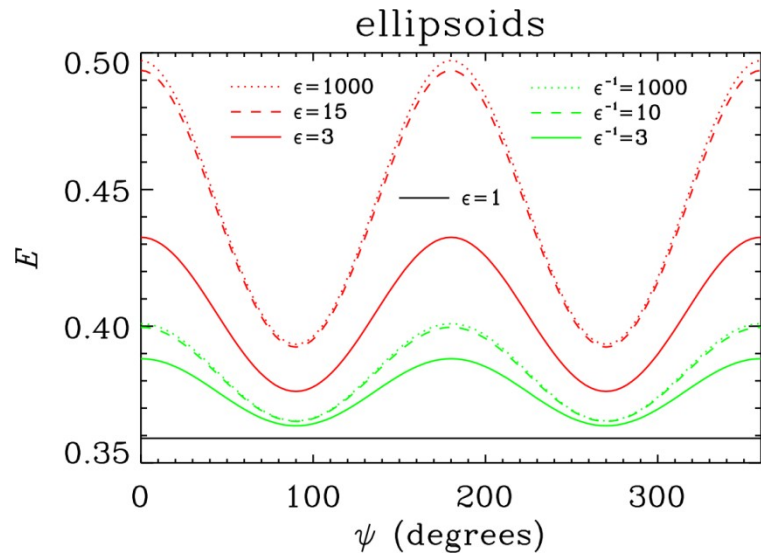
$$\sigma = \frac{E(\psi = 0^\circ)}{E(\psi = 90^\circ)}$$



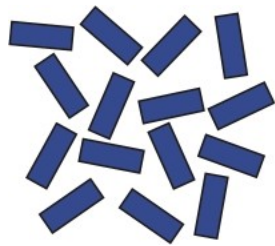
➤ An angular dependence in the $t_m \rightarrow \infty$ regime is a signature of CSA !

* Özarslan, J Magn Reson, 199, p. 56, 2009.

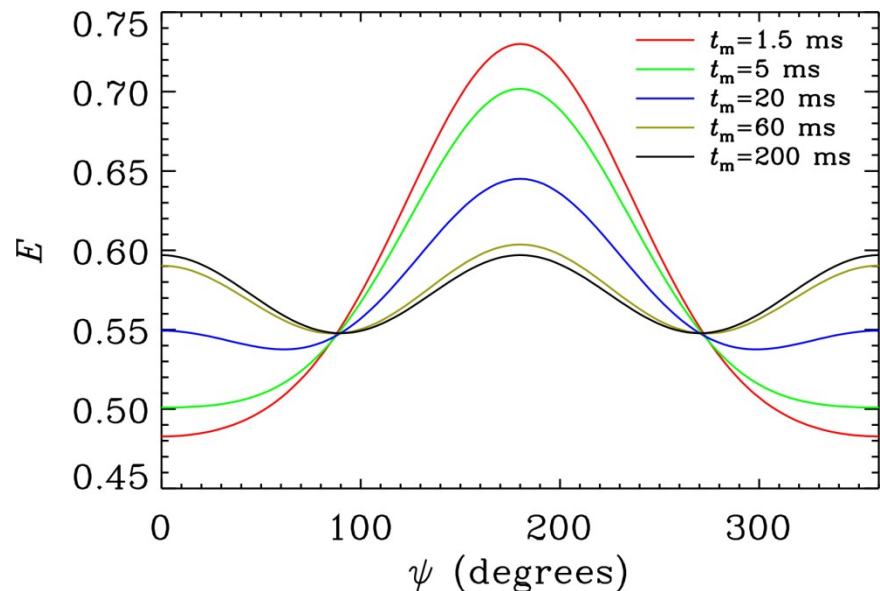
Signal Dependence on CSA



➤ There is a range of CSA values that can be extracted from the signal.



➤ Transition from μA to CSA



Conclusion

- Diffusion-weighted acquisitions can be used to characterize tissue microstructure without the need to employ high resolution imaging.
- Restricted diffusion models enable the extraction of structural features, such as cell size, shape, intracellular volume fraction, ...etc.
- It may be possible to capture the complexity of the tissue by employing a disordered media model.
- Double-PFG MR is a promising new technique.
 - Allows probing restricted diffusion using low gradient strengths.
 - The signal exhibits unique features; the technique is more informative than single-PFG.

Acknowledgments:

- Peter J. Basser
- Noam Shemesh
- Cheng Guan Koay
- Michal E. Komlosch
- Yoram Cohen
- Carlo Pierpaoli
- Timothy M. Shepherd
- Peter E. Thelwall
- Stephen J. Blackband

Thank you for your
attention !

This research was supported by the Eunice Kennedy Shriver National Institute of Child Health and Human Development (NICHD), National Institutes of Health (NIH).

